

Effective Field Theory Approach To $\vec{n} + \vec{p} \rightarrow d + \gamma$ At Threshold

Tae-Sun Park^{a,b,1}, Kuniharu Kubodera^{a,c,2}, Dong-Pil Min^{a,d,3}
 and
 Mannque Rho^{a,e,4}

^a *School of Physics, Korea Institute for Advanced Study, Seoul 130-012, Korea*

^b *Theory Group, TRIUMF, Vancouver, B.C., Canada V6T 2A3*

^c *Department of Physics and Astronomy, University of South Carolina
 Columbia, SC 29208, USA*

^d *Department of Physics, Seoul National University, Seoul 151-742, Korea*

^e *Service de Physique Théorique, CE Saclay, 91191 Gif-sur-Yvette, France*

Abstract

Previously, in an effective field theory formulated by us, we have carried out parameter-free calculations of a large number of low-energy two-nucleon properties. An experiment at the Institut Laue-Langevin is currently measuring spin-dependent effects in the polarized np capture process $\vec{n} + \vec{p} \rightarrow d + \gamma$ at threshold. Noting that spin-dependent observables for this reaction are sensitive to terms of chiral orders higher than hitherto studied, we extend our effective theory approach to this process and make *parameter-free predictions* on the spin-dependent observables.

¹E-mail: park@alpha02.triumf.ca

²E-mail: kubodera@sc.edu

³E-mail: dpmin@phya.snu.ac.kr

⁴E-mail: rho@spht.saclay.cea.fr

1 Introduction

An experiment by Müller *et al* [1] at the Institut Laue-Langevin (ILL) is currently measuring spin-dependent effects in the thermal neutron capture process

$$\vec{n} + \vec{p} \rightarrow d + \gamma, \quad (1)$$

wherein, as indicated, both the incident neutron and the target proton are polarized. At threshold, the initial nuclear state is in either the $^1S_0(T=1)$ or $^3S_1(T=0)$ channel, where T is the isospin. The process (1) therefore receives contributions from the isovector M1 matrix element (M1V) between the initial 1S_0 ($T=1$) and the final deuteron ($T=0$) state, along with the isoscalar M1 matrix element (M1S) and the isoscalar E2 (E2S) matrix element between the initial 3S_1 ($T=0$) and the final deuteron 3S_1 – 3D_1 states.^{#1} Since M1V is by far the largest amplitude (see below), the spin-averaged cross section $\sigma_{unpol}(np \rightarrow d\gamma)$ is totally dominated by M1V. Meanwhile, since the initial 1S_0 state has $J=0$, the M1V cannot yield spin-dependent effects, whereas M1S and E2S can. This means that, as first noted by Breit and Rustgi[3], the spin-dependent observables in (1) are sensitive to small isoscalar matrix elements. To explain the significance of this feature in the context of nuclear effective field theory (EFT), we first give a brief discussion of the “chiral filter hypothesis” [4].

The chiral filter hypothesis based on current algebra was proposed in 1978 prior to the advent of modern nuclear EFT. It dictates that corrections to the single-particle transitions in nuclei for the isovector M1 operator and the weak axial charge operator should be dominated by one-soft-pion-exchange two-body currents. It was shown in [5] that this dominance is naturally explained by chiral perturbation theory; the soft-pion exchange diagrams are leading-order two-body diagrams in chiral counting. A thorough nuclear EFT calculation of M1V carried out in [6] gave a precise, parameter-free estimate of σ_{unpol} , which was in perfect agreement with the experimental value [7]; furthermore, it was confirmed that the major corrections to the one-body (single-nucleon) current in M1V indeed come from one-soft-pion-exchange. For the axial charge also, its large enhancement due to the soft-pion exchange two-body currents is by now well established [8]. Thus, for the observables “protected” by the chiral filter (i.e., observables essentially determined by leading chiral-order terms), nuclear EFT has been highly successful.

The question now is whether we can profitably apply nuclear EFT to observables “unprotected” by the chiral filter. With leading chiral-order contributions vanishing, one must consider higher order diagrams, a task which can quickly become formidable. The above-mentioned isoscalar matrix elements, M1S and E2S, are examples of the “unprotected” observable. As is well known, the one-body contribution of M1S is highly suppressed due to the orthogonality between the initial 3S_1 and the final deuteron state. The soft-pion ex-

^{#1} The reason why E2S needs to be considered will be explained later in the text. We shall also discuss later the $E1$ contribution recently considered by Chen, Rupak and Savage [2].

change is also suppressed, there being no isoscalar $\mathcal{B}^\mu \pi NN$ vertex in the leading order chiral Lagrangian, where \mathcal{B}^μ is the external isoscalar field that couples to the baryonic current. Due to this double suppression, the size of M1S becomes even comparable (see below) to that of E2S, which is a higher-order multipole and hence, in normal circumstances, can be ignored. This situation suggests that we must go up to an unusually high chiral order before getting sensible estimates of the isoscalar matrix elements that govern the spin observables in (1). However, we show in this paper (confirming the previous results reported in [8]) that nuclear EFT allows us to make a systematic and reasonably reliable estimation of M1S and E2S.

By the very nature of EFT, an effective Lagrangian involves, at each order of power counting, a certain number of parameters. These parameters are in principle calculable from first principles for a given scale (*e.g.*, lattice QCD [9]) but, in practice, they have to be fixed by experimental data. Once the parameters are so fixed, the Lagrangian can then be used to make predictions for other processes governed by the same parameters. However, it often happens that after fixing the parameters there is not much room left for prediction. A major point of our work is to demonstrate that one can make a genuine EFT prediction even for the highly suppressed M1S and E2S. Our *bona fide* prediction not biased by pre-existing numbers can be tested soon by the forthcoming results from the ILL experiment [1].

2 Polarization observables

Adopting the convention of Müller et al [1], we write the transition amplitude as

$$\langle \psi_d, \gamma(\hat{k}, \lambda) | \mathcal{T} | \psi_{np} \rangle = \chi_d^\dagger \mathcal{M}(\hat{k}, \lambda) \chi_{np} \quad (2)$$

with

$$\begin{aligned} \mathcal{M}(\hat{k}, \lambda) = & \sqrt{4\pi} \frac{\sqrt{v_n}}{2\sqrt{\omega} A_s} \left[i(\hat{k} \times \hat{\epsilon}_\lambda^*) \cdot (\vec{\sigma}_1 - \vec{\sigma}_2) \text{M1V} \right. \\ & \left. - i(\hat{k} \times \hat{\epsilon}_\lambda^*) \cdot (\vec{\sigma}_1 + \vec{\sigma}_2) \frac{\text{M1S}}{\sqrt{2}} + (\vec{\sigma}_1 \cdot \hat{k} \vec{\sigma}_2 \cdot \hat{\epsilon}_\lambda^* + \vec{\sigma}_2 \cdot \hat{k} \vec{\sigma}_1 \cdot \hat{\epsilon}_\lambda^*) \frac{\text{E2S}}{\sqrt{2}} \right] \end{aligned} \quad (3)$$

where v_n is the velocity of the projectile neutron, A_s is the deuteron normalization factor $A_s \simeq 0.8850 \text{ fm}^{-1/2}$, and χ_d (χ_{np}) denotes the spin wave function of the final deuteron (initial np) state. The emitted photon is characterized by the unit momentum vector \hat{k} , the energy ω and the helicity λ , and its polarization vector is denoted by $\hat{\epsilon}_\lambda \equiv \hat{\epsilon}_\lambda(\hat{k})$. The amplitudes, M1V, M1S and E2S, represent the isovector M1, isoscalar M1 and isoscalar E2 contributions, respectively.^{#2} These quantities are defined in such a manner that they all have the dimension of length, and the cross section for the unpolarized np system takes the form

$$\sigma_{unpol} = |\text{M1V}|^2 + |\text{M1S}|^2 + |\text{E2S}|^2. \quad (4)$$

^{#2}These amplitudes are real at threshold.

As we shall see below, the isoscalar terms ($|M1S|^2$ and $|E2S|^2$) are strongly suppressed relative to $|M1V|^2$ — approximately by a factor of $\sim O(10^{-6})$ — so the unpolarized cross section is practically unaffected by the isoscalar terms. As mentioned, the isovector M1 amplitude was calculated [6] very accurately up to $\mathcal{O}(Q^3)$ relative to the single-particle operator. The result expressed in terms of M1V is: $M1V = 5.78 \pm 0.03$ fm, which should be compared to the empirical value $\sqrt{\sigma_{unpol}^{exp}} = 5.781 \pm 0.004$ fm. In this paper, therefore, we will focus on the isoscalar amplitudes.

The isoscalar matrix elements are given by

$$\begin{aligned} M1S &\equiv -\frac{\sqrt{2}\omega^{\frac{3}{2}}}{\sqrt{v_n}} \langle \psi_d^{J_z=1} | \mu^z | \psi_t^{J_z=1} \rangle, \\ E2S &\equiv \frac{\omega^{\frac{5}{2}}}{\sqrt{8}\sqrt{v_n}} \langle \psi_d^{J_z=1} | Q^{33} | \psi_t^{J_z=1} \rangle \end{aligned} \quad (5)$$

with

$$\begin{aligned} \vec{\mu} &= \frac{1}{2} \int d^3\vec{x} \vec{x} \times \vec{J}_{EM}(\vec{x}), \\ Q^{ij} &= \int d^3\vec{x} (3x^i x^j - \delta^{ij} \vec{x}^2) J_{EM}^0(\vec{x}), \end{aligned} \quad (6)$$

where $J_{EM}^\mu(\vec{x})$ is the EM current. The spin-triplet initial np and the final deuteron wavefunctions, $|\psi_t^{J_z}\rangle$ and $|\psi_d^{J_z}\rangle$, are given as

$$\langle \vec{r} | \psi_{t,d}^{J_z} \rangle \equiv \frac{1}{\sqrt{4\pi r}} \left[u_{t,d}(r) + \frac{S_{12}(\hat{r})}{\sqrt{8}} w_{t,d}(r) \right] \chi_{1J_z} \zeta_{00} \quad (7)$$

with the boundary conditions

$$\lim_{r \rightarrow \infty} u_d(r) = A_s e^{-\gamma_d r}, \quad \lim_{r \rightarrow \infty} u_t(r) = r - a_t, \quad (8)$$

and

$$\lim_{r \rightarrow \infty} \frac{w_d(r)}{u_d(r)} = \eta_d, \quad \lim_{r \rightarrow \infty} \frac{w_t(r)}{u_t(r)} = 0, \quad (9)$$

where $\gamma_d = \sqrt{B_d m_N}$ with $B_d \simeq 2.224575$ MeV the binding energy and $m_N \simeq 939$ MeV the nucleon mass; $\eta_d \simeq 0.0250$ is the asymptotic D/S ratio of the deuteron; $a_t \simeq 5.4192$ fm is the 3S_1 np scattering length, $S_{12}(\hat{r}) \equiv 3\vec{\sigma}_1 \cdot \hat{r} \vec{\sigma}_2 \cdot \hat{r} - \vec{\sigma}_1 \cdot \vec{\sigma}_2$, and $\chi(\zeta)$ is the spin (isospin) wavefunctions.

As mentioned, the spin-dependent observables are sensitive to the isoscalar matrix elements. Let $I_\lambda(\theta)$ be the angular distribution of photons with helicity $\lambda = \pm 1$, where θ is the angle between \hat{k} (direction of photon emission) and a quantization axis of nucleon polarization. For polarized neutrons with polarization \vec{P}_n incident on unpolarized protons, the photon circular polarization P_γ is defined by

$$P_\gamma \equiv \frac{I_{+1}(0^\circ) - I_{-1}(0^\circ)}{I_{+1}(0^\circ) + I_{-1}(0^\circ)}. \quad (10)$$

At threshold^{#3}, P_γ is given by

$$P_\gamma = |\vec{P}_n| \frac{\sqrt{2}(\mathcal{R}_{M1} - \mathcal{R}_{E2}) + \frac{1}{2}(\mathcal{R}_{M1} + \mathcal{R}_{E2})^2}{1 + \mathcal{R}_{M1}^2 + \mathcal{R}_{E2}^2} \quad (11)$$

where we have defined the ratios

$$\mathcal{R}_{M1} \equiv \frac{M1S}{M1V}, \quad \mathcal{R}_{E2} \equiv \frac{E2S}{M1V}. \quad (12)$$

When both protons and neutrons are polarized (along a common quantization axis) with polarizations \vec{P}_p and \vec{P}_n , respectively, the anisotropy η_γ is defined by

$$\eta_\gamma \equiv \frac{I(90^\circ) - I(0^\circ)}{I(90^\circ) + I(0^\circ)}, \quad (13)$$

where $I(\theta) = I_{+1}(\theta) + I_{-1}(\theta)$ is the angular distribution of total photon intensity (regardless of their helicities). At threshold, we have

$$\eta_\gamma = pP \frac{\mathcal{R}_{M1}^2 + \mathcal{R}_{E2}^2 - 6\mathcal{R}_{M1}\mathcal{R}_{E2}}{4(1 - pP) + (4 + pP)(\mathcal{R}_{M1}^2 + \mathcal{R}_{E2}^2) + 2pP\mathcal{R}_{M1}\mathcal{R}_{E2}} \quad (14)$$

where

$$pP \equiv \vec{P}_p \cdot \vec{P}_n. \quad (15)$$

We note that P_γ is linear in \mathcal{R} 's in the leading order. By contrast, unless $pP \sim 1$, the anisotropy η_γ is quadratic in \mathcal{R} 's and hence highly suppressed. For $pP \sim 1$ (nearly perfect polarization), η_γ becomes $\mathcal{O}(1)$ in powers of \mathcal{R} 's and can be of a substantial magnitude. This feature suggests the possibility of obtaining two independent constraints on \mathcal{R} 's, one from P_γ and the other from η_γ , which would allow extraction of the individual values of \mathcal{R}_{M1} and \mathcal{R}_{E2} . There exist data on P_γ due to Bazhenov *et al.* [10], and the ILL experiment [1] is expected to give information on η_γ .

Our argument above is based on the strict threshold kinematics. A few remarks are in order here. When the velocity of the projectile neutron v_n goes to zero, the cross section diverges as v_n^{-1} and consequently the matrix elements as $v_n^{-\frac{1}{2}}$. However, the quantity that is actually measured in experiment is the yield, the flux times the cross section. Since the flux is proportional to v_n , $v_n\sigma$ near threshold is constant with good accuracy, and one measures the thermal average of this v_n -independent yield. It is customary to translate the measured yield into the cross sections using a fixed velocity, $v_n = 2200$ m/s, which corresponds to the average neutron velocity at room temperature. We adopt this convention throughout this paper, and we mean by “at threshold” that we are neglecting any higher order corrections in v_n . Chen et al.[2] pointed out that at this velocity the isovector E1 matrix element (we denote it by E1V) connecting initial 3P_J waves with the deuteron state can compete with M1S and E2S. They calculated P_γ including the E1V contribution but the corresponding

^{#3}See below for a caveat on the kinematics of the experiments.

result for η_γ has not been reported. The inclusion of E1V affects the asymmetry $A_{\eta_m}^\gamma(\theta)$ defined and calculated in [2]. However, for photons emitted in the $\theta = 0$ direction, there is no contribution from E1V. This means that P_γ , eq.(10), is not influenced at all by the E1V contribution. Meanwhile, according to [2], η_γ arising from E1V has a very different pP dependence from that arising from M1S and E2S. In principle, therefore, it should be possible to distinguish experimentally these two η_γ 's of different origins. In the present work limited to the threshold kinematics, we do not discuss the contribution of E1V.^{#4}

3 ChPT calculation

The chiral counting rules relevant to electroweak vertices in two-nucleon systems are well known by now (see, e.g., [6]). The chiral index ν of a given irreducible diagram is given by

$$\nu = 1 - 2C + 2L + \sum_i \nu_i, \quad \nu_i = d_i + e_i + \frac{n_i}{2} - 2, \quad (16)$$

where C is the number of disjoint pieces ($C = 2$ for one-body currents and $C = 1$ for two-body currents), and L the number of loops; d_i , e_i and n_i are, respectively, the numbers of derivatives/ m_π 's, external fields and nucleon lines at the i -th vertex. Since chiral symmetry guarantees $\nu_i \geq 0$, eq.(16) implies that the one-body EM current J_{1B}^μ starts at $\mathcal{O}(Q^{-3})$ while the two-body current J_{2B}^μ starts at $\mathcal{O}(Q^{-1})$. As spelled out in [6], there are additional suppression factors of either a kinematical or symmetry origin. For instance, the space-part of the one-body current is suppressed by one power in Q relative to its time part. The detailed counting rules for the two-body isoscalar EM current are rather complicated and will be discussed later.

At present, there are essentially two “alternative” ways of power counting in setting up an effective field theory for two-nucleon systems. One is the original Weinberg scheme [11], in which the leading four-Fermi contact interaction and a pion-exchange are treated on the same footing in calculating the “irreducible” graphs for a potential that is to be iterated to all orders in the “reducible” channel. The power counting is done only for irreducible vertices. The other is the “power divergence subtraction” (PDS) scheme [12], in which only the leading (nonderivative) four-Fermi contact interaction is iterated to all orders, with the higher-order contact interactions and the pion exchange treated perturbatively. While the PDS scheme is perhaps more systematic in power counting, we believe that the Weinberg scheme is not only consistent with the strategy of EFT but also, in the sense developed below, more flexible and predictive with possible errors due to potential inconsistency in power counting generically suppressed. In our work we adopt the Weinberg scheme. In this framework, the power counting for electroweak transition amplitudes simply reduces

^{#4} In connection to the above-mentioned thermal averaging, we note that the ratio E1V/M1V is proportional to v_n , while \mathcal{R}_{M1} and \mathcal{R}_{E2} are v_n -independent.

to chiral counting in the irreducible vertex for the current, as the current appears only once in the graphs. We are then allowed to separate the current matrix element into the one-body (single-particle) and two-body (exchange-current) terms. This framework has the advantage that it can be straightforwardly applied to n -body systems for $n > 2$.

Iterating the irreducible vertex to all orders in the reducible channel is equivalent to solving the Schrödinger equation with a corresponding potential. This then suggests that we use, in calculating nuclear responses to slowly varying electroweak probes, those wave functions computed with so-called phenomenological “realistic potentials”. A prime example of these realistic potentials is the Argonne v_{18} potential [13] (called in short Av18). Thus in this approach, referred to as the *hybrid approach*, the one-body and two-body transition operators derived from EFT are sandwiched between the initial and final two-nucleon wavefunctions distorted by a phenomenological N-N potential. This procedure of mapping effective field theory to realistic wave functions has recently been justified by means of a cutoff regularization [14]. A similar argument in support of such a hybrid procedure has been presented by van Kolck [15].

Previously we adopted this scheme to study the unpolarized $p(n, \gamma)d$ reaction for the thermal neutron. The cross section for this process was computed to next-to-next-to-leading order (NNLO) in the above-described chiral counting scheme for the transition vertex [6], and with the use of the Av18 wave functions. The resulting theoretical cross section, $\sigma_{unpol}^{th} = 334 \pm 3$ mb, agrees very well with the experimental value $\sigma_{unpol}^{exp} = 334.2 \pm 0.5$ fm [7]; σ_{unpol}^{th} consists of the leading 1-body contribution, 305.6 mb, and the 2-body exchange-current contribution, which in conformity with the chiral filter is dominated by the soft one-pion exchange.

As shown in [14], the single-particle matrix element has negligible uncertainty, and therefore the theoretical error is entirely attributable to the uncertainty in the exchange-current operator associated with the short-distance part of the interactions. This short-range behavior is not fully controlled in the formulation of [14]. The short-distance part introduces a scale and renormalization-scheme dependence, and only those results that are not sensitive to this uncertainty can be trusted. In a framework that uses realistic wave functions, the short-distance scale is set by a (momentum) cutoff proportional to r_c^{-1} , where r_c is the “hard-core radius” that removes the part of the wave function for $r \lesssim r_c \neq 0$. The net effect of this cutoff is that in addition to cutting the radial integrals in the coordinate space, it removes *all* zero-range terms in the current operator including zero-ranged counter terms. After the four-fermion counter term is removed by the hard core, there are no more parameters in the theory ^{#5}. This procedure, familiar to nuclear physicists, may be viewed as a form of exploiting the scheme dependence. We shall refer to this procedure as the hard-core cutoff scheme (HCCS). HCCS can be justified for the process in question by

^{#5}See appendix B in the second reference of [6] for the zero-ranged counter term in question. In the framework of [12], which avoids scheme dependence at the expense of predictivity, this counter term plays a much more pronounced role, rendering a *bona fide* prediction infeasible [16].

using a (momentum) cutoff $\sim r_c^{-1}$ and showing that the counter-term contribution “killed” by the hard core lies within that uncertainty range.^{#6} The 1% theoretical error assigned to σ_{unpol}^{th} above represents uncertainty in this cutoff procedure. We will see below that, when the chiral filter does not apply, the removal of the zero-range counter terms by the simple hard-core cutoff may be much less reliable.

3.1 One-Body Contributions

Either starting from the well-known EM form factors of the nucleon, or carrying out an explicit ChPT calculation that reproduces the form factors, we arrive at the following expressions for the one-body operators:

$$\begin{aligned}\vec{\mu}_{1B}(\vec{r}_1, \vec{r}_2) &= \frac{e}{2m_N} \sum_{i=1,2} \left[\frac{1 + \tau_i^z}{2} \vec{r}_i \times \vec{p}_i + \frac{\mu_S + \tau_i^z \mu_V}{2} \vec{\sigma}_i \right. \\ &\quad \left. - \frac{1 + \tau_i^z}{2} \frac{(\vec{\sigma}_i \vec{p}_i^2 - \vec{p}_i \vec{\sigma}_i \cdot \vec{p}_i)}{4m_N^2} + \mathcal{O}\left(\frac{\vec{p}_i^2}{m_N^2}\right) \right], \\ Q_{1B}^{ab}(\vec{r}_1, \vec{r}_2) &= e \sum_{i=1,2} \left[\left(3r_i^a r_i^b - \delta^{ab} r_i^2 \right) \frac{1 + \tau_i^z}{2} \left(1 + \frac{\vec{p}_i^2}{2m_N^2} \right) \right. \\ &\quad \left. + \frac{(2\mu_S - 1) + (2\mu_V - 1)\tau_i^z}{4m_N^2} U_i^{ab} + \mathcal{O}\left(\frac{\vec{p}_i^2}{m_N^4}\right) \right] \end{aligned} \quad (17)$$

with

$$U_i^{ab} \equiv \frac{3}{2} r_i^a (\vec{p}_i \times \vec{\sigma}_i)^b + \frac{3}{2} r_i^b (\vec{p}_i \times \vec{\sigma}_i)^a - \delta^{ab} \vec{r}_i \cdot (\vec{p}_i \times \vec{\sigma}_i), \quad (18)$$

where $\mu_S \simeq 0.87981$ and $\mu_V \simeq 4.70589$. The matrix elements (5) can then be obtained by a straightforward calculation. For example, the leading order one-body matrix elements are given by

$$\begin{aligned}M1S_{1B}^{LO} &= -\frac{\sqrt{2}e\omega^{\frac{3}{2}}}{2\sqrt{v_n}m_N} \int_0^\infty dr \left[\frac{3}{4} w_d(r) w_t(r) + \mu_S \left(u_d(r) u_t(r) - \frac{w_d(r) w_t(r)}{2} \right) \right], \\ E2S_{1B}^{LO} &= \frac{e\omega^{\frac{5}{2}}}{20\sqrt{v_n}} \int_0^\infty dr r^2 \left[\frac{u_d(r) w_t(r) + w_d(r) u_t(r)}{2} - \frac{w_d(r) w_t(r)}{\sqrt{8}} \right]. \end{aligned} \quad (19)$$

As mentioned earlier, the one-body M1S is suppressed by the orthogonality

$$\int_0^\infty dr [u_d(r) u_t(r) + w_d(r) w_t(r)] = 0. \quad (20)$$

Using the Av18 wavefunctions, the numerical results for the sum of the LO and NLO are given as

$$\begin{aligned}M1S_{1B}(\text{fm}) &= (-4.192 - 0.105) \times 10^{-3} = -4.297 \times 10^{-3}, \\ E2S_{1B}(\text{fm}) &= (1.401 - 0.007) \times 10^{-3} = 1.394 \times 10^{-3}. \end{aligned} \quad (21)$$

^{#6} Since our calculations are carried out in coordinate space, r_c is related to the hard-core radius used in standard nuclear physics calculations.

We see that the size of the one-body M1S is about 10^3 times smaller than M1V, a suppression which can be traced to the above-mentioned orthogonality and the smallness of μ_S as compared to μ_V .

3.2 Two-body contributions

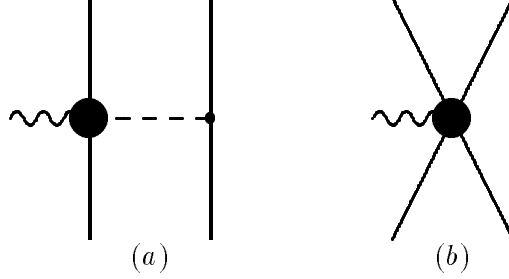


Figure 1: Generic diagrams for the two-body isoscalar current. The solid circles include counter-term insertions and (one-particle irreducible) loop corrections. The wiggly line stands for the external field (current) and the dashed line the pion. One-loop corrections for the pion propagator and the πNN vertex need to be included at the same order.

Generic diagrams for the two-body isoscalar current are depicted in Fig. 1. All the propagators and the vertices therein should be understood as the renormalized quantities that include all the loops and counter term insertions to a given order. The vertices with non-trivial renormalization are represented by big filled circles. The one-loop graphs relevant to the filled circle in Fig. 1a (Fig.1b) are drawn in Fig. 2 (Fig. 3).

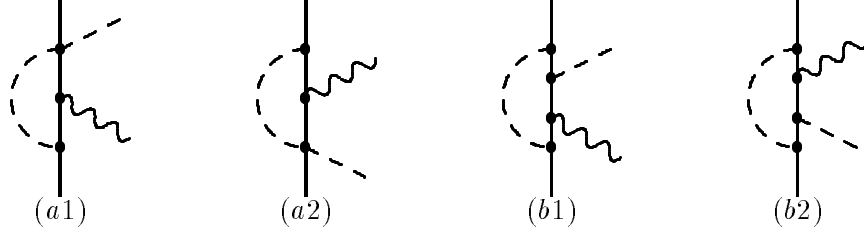


Figure 2: One-loop graphs that contribute to the $\mathcal{B}^\mu \pi NN$ vertex, \mathcal{B}^μ representing the external isoscalar field. These diagrams give rise to corrections of $\mathcal{O}(Q^4)$ and higher orders to the leading-order one-body term.

We now proceed to discuss in detail the counting rules for the two-body contributions. For easy reference, we let $N^n\text{LO}$ stand for contributions of order $\mathcal{O}(Q^n)$ relative to the leading one-body term. For the chiral-filter protected M1V, since the isovector $\gamma\pi NN$ vertex with $\nu_i = 0$ enters at the blob of Fig. 1a, the leading correction appears at $N^1\text{LO}$ and the one-loops and the counter-terms appear at $N^3\text{LO}$. For the isoscalar current, not protected by the chiral filter, the counting rules are quite different. The $\mathcal{B}^\mu \pi NN$ coupling

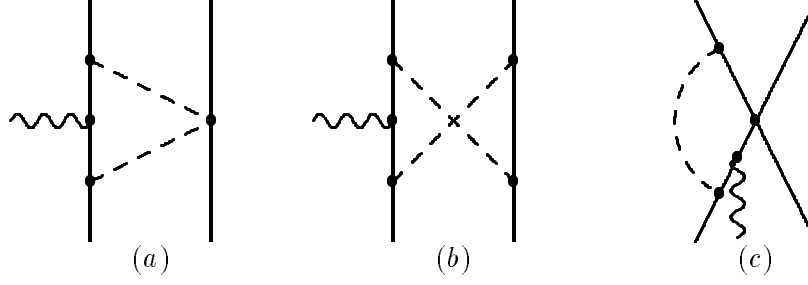


Figure 3: One-loop graphs contributing to the two-body baryonic currents. They come at $\mathcal{O}(Q^4)$ and higher orders relative to the LO one-body term. All possible insertions on the external line are understood.

is highly suppressed by chiral symmetry, and its first non-vanishing term appears at

$$\nu_i(\mathcal{B}^i \pi NN) \geq 2, \quad \nu_i(\mathcal{B}^0 \pi NN) \geq 3. \quad (22)$$

The same suppression factors appear in the contact $\mathcal{B}^\mu NNNN$ vertex. As a result, leading corrections for the M1S are $N^3\text{LO}$, which arise from a chiral Lagrangian [17, 6] of the form

$$\begin{aligned} \mathcal{L}_2 = & -\frac{g_\rho^2}{8\pi^2 m_\rho^2} \epsilon^{\mu\nu\alpha\beta} (\partial_\alpha \mathcal{B}_\beta - \partial_\beta \mathcal{B}_\alpha) \bar{B}_v v_\mu i \Delta_\nu B_v \\ & - ig_4 (\partial_\mu \mathcal{B}_\nu - \partial_\nu \mathcal{B}_\mu) \bar{B}_v [S_v^\mu, S_v^\nu] B_v \bar{B}_v B_v \end{aligned} \quad (23)$$

where B_v is the nucleon field; the definitions of the four-velocity v^μ , the spin-operator S_v^μ and the covariant pion-derivative Δ^μ can be found in [6]. Although the second term contains an unknown constant g_4 , the first term is free from an additional parameter, for it is given by the Wess-Zumino term (related to the Adler-Bell-Jackiw anomaly) the strength of which can be determined from the KSFR relation. There is also a Lagrangian consisting of $1/m$ corrections that we shall refer to as the “fixed-term” Lagrangian in which all the coefficients are uniquely determined [17],

$$\mathcal{L}^{\text{fixed}} = \bar{B}_v \left[\frac{g_A}{m_N} \{S_v \cdot D, v \cdot \Delta\} - \frac{g_A}{4m_N^2} (iS_v \cdot \Delta D^2 + 2iS_v \cdot \overleftarrow{D} \Delta \cdot D + \text{h.c.}) + \dots \right] B_v \quad (24)$$

where $g_A \simeq 1.26$ is the axial coupling constant and the ellipses denote terms irrelevant to our present study. The chiral index of the first term is $\nu_i = 1$, while all the other terms have $\nu_i = 2$. It is to be noted, however, that the $\nu_i = 1$ term is proportional to the energy-transfer,^{#7} which is of order of Q^2/m_N . Consequently all the terms in eq.(24) give $N^3\text{LO}$ contributions to the M1 operators. There is no counter-term contribution to E2S up to $N^4\text{LO}$ with which we are concerned.

The loop contributions enter at $N^4\text{LO}$ and are finite. Usually, counter-term contributions enter – regardless of whether the loops are divergent or not – at the same order as the

^{#7} We have replaced the energy transfer $v \cdot q_i = p_i^0 - p_i^0$ by $\frac{\vec{p}_i^2}{2m_N} - \frac{\vec{p}_i^2}{2m_N}$, where the subscript i is the particle index.

loop contributions. In our case, however, there is no counter term contribution. Additional parameters characterizing the nuclear potential appear at the four-fermion vertex in Fig. 3c, through a Lagrangian of the form

$$\mathcal{L}_0 = -\frac{1}{2} \sum_A C_A (\bar{B} \Gamma_A B)^2. \quad (25)$$

Here Γ_A 's stand for non-derivative operators, and C_A are constant coefficients. Due to the Fermi-Dirac statistics, only two of the four possible C_A are independent.

Summing all the two-body contributions up to N⁴LO and Fourier-transforming the resulting expressions into coordinate space, we obtain the following isoscalar M1 and E2 operators:

$$\begin{aligned} \vec{\mu}_{2B}(\vec{r}) &= \frac{e}{2m_N} \left[\frac{1}{4} \{ \vec{L}, S_{12}(\hat{r}) \} \tilde{C}_1^T(r) + \frac{1}{2} \vec{L} \tilde{C}_2(r) \right. \\ &\quad + \left(3\hat{r} \hat{r} \cdot \vec{S} - \vec{S} \right) \left(\mu_S \tilde{C}_3^T(r) + \frac{r}{12} \tilde{C}_5^V(r) \right) \\ &\quad \left. + \vec{S} \left(\mu_S \tilde{C}_4(r) - \frac{1}{6} \tilde{C}_5^V(r) \right) \right] + \vec{\mu}_{1\pi}^{\text{fixed}}(\vec{r}), \end{aligned} \quad (26)$$

$$Q_{2B}^{ij}(\vec{r}) = \frac{e}{4} \left(3r^i r^j - \delta^{ij} r^2 \right) \left[S_{12}(\hat{r}) \tilde{C}_1^T(r) + \tilde{C}_2(r) \right] \quad (27)$$

where $\vec{S} \equiv \frac{1}{2}(\vec{\sigma}_1 + \vec{\sigma}_2)$ and \vec{L} is the orbital angular momentum operator for the relative motion. We have separated the contribution from the fixed-term Lagrangian (24),

$$\begin{aligned} \vec{\mu}_{1\pi}^{\text{fixed}}(\vec{r}) &= \frac{e}{2m_N} \frac{\tau_1 \cdot \tau_2 m_\pi^3 g_A^2}{16m_N f_\pi^2} \left[\left(\frac{4}{3} \vec{\mathcal{E}}(\vec{p}) - \frac{\vec{\sigma}_1 \cdot \vec{\sigma}_2}{3} \vec{L} \right) \left[y_0(m_\pi r) - \delta^3(m_\pi \vec{r}) \right] \right. \\ &\quad \left. + \left(3\vec{\mathcal{E}}(\hat{r} \hat{r} \cdot \vec{p}) - \frac{4}{3} \vec{\mathcal{E}}(\vec{p}) - \frac{\{S_{12}(\hat{r}), \vec{L}\}}{6} \right) y_2(m_\pi r) \right] \end{aligned} \quad (28)$$

with

$$\mathcal{E}^i(\vec{X}) = \epsilon^{ijk} r^j \frac{\sigma_1^k \sigma_2^l + \sigma_2^k \sigma_1^l}{2} X^l, \quad (29)$$

where \vec{X} is either \vec{p} or $\hat{r} \hat{r} \cdot \vec{p}$; $y_0(x) \equiv \frac{e^{-x}}{4\pi x}$ and $y_2(x) \equiv \left(1 + \frac{3}{x} + \frac{3}{x^2}\right) y_0(x)$ are Yukawa functions, and $\vec{p} \equiv -\frac{i}{2}(\vec{\nabla} - \overleftarrow{\nabla})$ is the momentum operator with the understanding that the derivatives act only on wavefunctions. The \tilde{C} 's are given as

$$\begin{aligned} \tilde{C}_1^T(r) &= \frac{N_1 m_\pi^3 e^{-m_\pi r}}{3} \left(1 + \frac{3}{m_\pi r} + \frac{3}{m_\pi^2 r^2} \right) + \frac{N_3 m_\pi^3}{24\pi r} \int_0^1 \frac{dz}{(z\bar{z})^2} K_3(x), \\ \tilde{C}_3^T(r) &= \left[\frac{2m_N}{\mu_S m_\pi} N_{\text{WZ}} - N_1 \right] m_\pi^3 \frac{e^{-m_\pi r}}{4\pi r} \left(1 + \frac{3}{m_\pi r} + \frac{3}{m_\pi^2 r^2} \right) - \frac{N_3 m_\pi^3}{8\pi r} \int_0^1 \frac{dz}{(z\bar{z})^2} K_3(x) \\ &\quad + \frac{m_\pi^3}{2\pi r} \int_0^1 \frac{dz}{z\bar{z}} \left[-\frac{4N_2}{3} K_3(x) + \frac{N_3}{6} x K_4(x) \right], \\ \tilde{C}_5^V(r) &= \frac{N_2 m_\pi^3}{\pi r} \int_0^1 \frac{dz}{z\bar{z}} K_3(x) \end{aligned} \quad (30)$$

and

$$\begin{aligned}
\tilde{C}_2(r) &= \vec{\sigma}_1 \cdot \vec{\sigma}_2 \frac{N_1 m_\pi^3}{3} \frac{e^{-m_\pi r}}{4\pi r} - \frac{N_2 m_\pi^3}{\pi r} \int_0^1 \frac{dz}{z\bar{z}} K_3(x) + V_1 \delta(\vec{r}) \\
&+ \frac{N_3 m_\pi^3}{24\pi r} \left\{ 3 \int_0^1 \frac{dz}{z\bar{z}} [6K_3(x) + 8K_1(x) + xK_0(x)] \right. \\
&\quad \left. - (3 + 2\vec{\sigma}_1 \cdot \vec{\sigma}_2) \int_0^1 \frac{dz}{(z\bar{z})^2} \frac{K_3(x) + 7K_1(x)}{4} \right\}, \\
\tilde{C}_4(r) &= \left[\frac{2m_N}{\mu_S m_\pi} N_{\text{WZ}} - N_1 \right] m_\pi^3 \frac{e^{-m_\pi r}}{4\pi r} + \frac{N_2 m_\pi^3}{3\pi r} \int_0^1 \frac{dz}{z\bar{z}} K_3(x) + \left[\frac{2m_N}{\mu_S} (N_{\text{WZ}} + g_4) + V_2 \right] \delta(\vec{r}) \\
&+ \frac{N_3 m_\pi^3}{24\pi r} \left\{ \frac{1}{2} \int_0^1 \frac{dz}{z\bar{z}} [9K_3(x) + 15K_1(x) + 2xK_0(x)] - 3 \int_0^1 \frac{dz}{(z\bar{z})^2} \frac{K_3(x) + 7K_1(x)}{4} \right\}
\end{aligned} \tag{31}$$

where $x \equiv \frac{m_\pi r}{\sqrt{z\bar{z}}}$, $\bar{z} \equiv (1 - z)$ and $K_\nu(x)$ is the irregular modified Bessel functions^{#8} of order ν . The coefficients N 's are defined by

$$\begin{aligned}
N_1 &= \tau_1 \cdot \tau_2 \frac{g_A^4}{128\pi f_\pi^4}, \\
N_2 &= \tau_1 \cdot \tau_2 \frac{g_A^2}{128\pi f_\pi^4}, \\
N_3 &= (3 + 2\tau_1 \cdot \tau_2) \frac{g_A^4}{128\pi f_\pi^4}, \\
N_{\text{WZ}} &= \tau_1 \cdot \tau_2 \frac{g_A g_\rho^2}{48\pi^2 f_\pi^2 m_\rho^2},
\end{aligned} \tag{32}$$

and V_1 and V_2 are two independent coefficients involving C_A ,

$$\begin{aligned}
V_1 &\equiv -\vec{\sigma}_1 \cdot \vec{\sigma}_2 \frac{N_1 m_\pi}{3} + \frac{g_A^2 m_\pi}{64\pi f_\pi^2} \sum_A \left(\tau_1^b \sigma_1^j C_A \Gamma_A \Gamma_A \tau_1^b \sigma_1^j + (1 \leftrightarrow 2) \right), \\
(\vec{\sigma}_1 + \vec{\sigma}_2) V_2 &\equiv N_1 m_\pi (\vec{\sigma}_1 + \vec{\sigma}_2) + \frac{g_A^2 m_\pi}{64\pi f_\pi^2} \sum_A \left(\tau_1^b \sigma_1^j \{C_A \Gamma_A \Gamma_A, \sigma_1\} \tau_1^b \sigma_1^j + (1 \leftrightarrow 2) \right)
\end{aligned} \tag{33}$$

In the above equations, the terms with g_4 and N_{WZ} as well as the fixed-terms are due to N³LO contributions, while all the other terms come from N⁴LO contributions. Fortunately, the parameters V_2 can be absorbed into g_4 ,^{#9}

$$g_4 \rightarrow g'_4 \equiv g_4 + N_{\text{WZ}} + \frac{\mu_S}{2m_N} V_2. \tag{35}$$

The V_1 term, which in naive counting is N⁴LO, is further suppressed and plays little role. The reason is not hard to understand: V_1 appears only in $\tilde{C}_2(r)$, which is accompanied

^{#8} We follow the definition of the Bessel functions given in [18].

^{#9} Similarly, N_{WZ} can be renormalized to absorb some N⁴LO contribution,

$$N_{\text{WZ}} \rightarrow N'_{\text{WZ}} \equiv N_{\text{WZ}} - \frac{\mu_S m_\pi}{2m_N} N_1. \tag{34}$$

Unlike the g_4 case, however, this does not reduce the number of unknown parameters, since the value of N_1 is already known.

either by \vec{L} (for M1S) or by r^2 (for E2S). As a consequence, the V_1 term contribution has the form

$$\sim V_1 \int d^3\vec{r} r^n \delta^3(\vec{r}), \quad (36)$$

where $n = 4$ (for M1S) and $n = 2$ (for E2S), and eq.(36) is obviously zero. Thus we are left with only one parameter g'_4 . In the next section we will show that we can fix g'_4 by taking the magnetic moment of the deuteron as input. This will enable us to make a totally parameter-free prediction for the ILL experiment.

4 Renormalization

The two-body contribution to the M1S, denoted by M1S_{2B}, can be expressed as

$$\text{M1S}_{2B} = \int_0^\infty dr \mathcal{F}_t(r) - \frac{\sqrt{2}e\omega^{\frac{3}{2}}}{\sqrt{v_n}} g'_4 \int d^3\vec{r} \frac{u_d(r)u_t(r)}{4\pi r^2} \delta^{(3)}(\vec{r}), \quad (37)$$

where $\mathcal{F}_t(r)$ consists of $\tilde{C}(r)$'s [see eqs.(30, 31)] and the final and initial radial wavefunctions. The first integral diverges since $\mathcal{F}_t(r)$ contains a piece which behaves like $1/r^2$ for $r \rightarrow 0$. If the hard-core cutoff scheme (HCCS) defined earlier can be used, this divergence simply disappears, as the hard-core kills any contributions from $r < r_c$ (r_c = hard-core radius). A hard-core would remove altogether the second integral in eq.(37). HCCS was applied quite successfully to chiral-filter-protected quantities, e.g., M1V [6]. The numerical results in [6] exhibit only slight r_c -dependence, a feature that assures the predictivity of HCCS. For processes not protected by the chiral-filter, however, there is no reason to believe that HCCS continues to be satisfactory. This is because two-body corrections for these processes come from “short-ranged physics,” and therefore imposing a hard-core will throw out the main part of the relevant physics. For the process (1) this problem becomes even more serious because the strong suppression of the one-body M1S in our case means that even small changes in the two-body contributions can have a significant influence on the total transition amplitude. In particular, since we are calculating up to N⁴LO, it is not justifiable to neglect by fiat the g'_4 term, which is N³LO.

For systematic evaluation of the short-ranged contributions along with long-ranged contributions, a transparent method would be to impose a momentum cutoff $\Lambda \sim r_c^{-1}$ in performing Fourier transformation. This scheme would allow us to include in a well-defined manner the contributions from $r < r_c$, whereas they are simply thrown away in HCCS. Technically, however, it is cumbersome to introduce a cutoff in Fourier transformation. Fortunately, for our present purposes, we can use a convenient scheme equivalent to, but simpler than, the momentum cutoff method. For this scheme, we first note that, the large- r contributions being scheme-independent, only the contributions $r \lesssim r_c$ involve scheme-dependence. Secondly, while $\mathcal{F}_t(r)$ contains both the D -wave and S -wave radial functions, the terms involving the D -wave have higher powers of r and hence receive only minor

contributions from the small r region. Then the only quantity that is sensitive to the renormalization scheme is the small- r contribution of the term containing $u_d(r)$ and $u_t(r)$. For small r , however, these radial functions can be approximated as $u_d(r) \simeq u'_d(0)r$ and $u_t(r) \simeq u'_t(0)r$. The small- r contribution ($0 \leq r < r_c$) of the first integral of eq.(37) then can be written as

$$\int_0^{r_c} dr \mathcal{F}_t \simeq u'_d(0)u'_t(0)A \quad (38)$$

where A is an r_c -dependent but wavefunction-independent constant. This contribution can be absorbed into the redefinition of the parameter g'_4 ; the resulting g'_4 will become r_c -dependent. The net effect of this procedure is to remove the $r < r_c$ contribution while retaining the r_c -dependent g'_4 term. Operationally, we can achieve the same goal by replacing the delta function attached to g'_4 with the delta-shell function,

$$\delta^3(\vec{r}) \rightarrow \frac{\delta(r - r_c)}{4\pi r_c^2}. \quad (39)$$

For a given value of r_c we can fix g'_4 by fitting the deuteron magnetic moment. We shall call this scheme the modified hard-core cutoff scheme (MHCCS). A regularization scheme similar to MHCCS has often been used in the literature (see, for example, [19]). Hereafter we drop the prime on g'_4 for simplicity.

In MHCCS, eq.(37) is rewritten as

$$\text{M1S}_{2\text{B}} = \int_{r_c}^{\infty} dr \mathcal{F}_t(r) - \frac{\sqrt{2}\epsilon\omega^{\frac{3}{2}}}{\sqrt{v_n}} g_4 \frac{u_d(r_c)u_t(r_c)}{4\pi r_c^2} \equiv \text{M1S}_{2\text{B}}^{\text{finite}} + \text{M1S}_{2\text{B}}^{\text{zero}}. \quad (40)$$

We determine g_4 through the renormalization condition for the deuteron magnetic moment,

$$\mu_{d,2\text{B}} = \int_{r_c}^{\infty} dr \mathcal{F}_d(r) + 2m_N g_4 \frac{u_d^2(r_c)}{4\pi r_c^2} = \mu_d^{\text{exp}} - \mu_{d,1\text{B}}, \quad (41)$$

$$g_4 = \frac{1}{2m_N} \frac{4\pi r_c^2}{u_d^2(r_c)} \Delta\mu_d, \quad (42)$$

$$\Delta\mu_d \equiv \mu_d^{\text{exp}} - \mu_{d,1\text{B}} - \mu_{d,2\text{B}}^{\text{finite}} \quad (43)$$

For $r_c = 0.01, 0.2, 0.4, 0.6$ and 0.8 fm, we find $\Delta\mu_d = 0.024, 0.020, 0.022, 0.023$ and 0.023 (in units of the nuclear magneton); the corresponding values of g_4 are: $g_4(\text{fm}^4) = 5.06, 2.24, 0.73, 0.31$ and 0.20 . In Table 1 we give the renormalized M1S and its breakdown into the various individual contributions, for different values of r_c spanning a wide range, $0.01 \text{ fm} \leq r_c \leq 0.8 \text{ fm}$. We see that, while the finite part exhibits some r_c -dependence, the total M1S is completely insensitive to the value of r_c , owing to the renormalization to fit the magnetic moment of the deuteron. Our results can be summarized as

$$\text{M1S} = (-2.85 \pm 0.01) \times 10^{-3} \text{ fm}, \quad (44)$$

r_c (fm)	0.01	0.2	0.4	0.6	0.8
$M1S_{2B}^{WZ}(N^3LO)$	-3.384	-3.352	-3.197	-2.789	-2.159
$M1S_{2B}^{fixed}(N^3LO)$	-0.938	-0.941	-0.920	-0.823	-0.643
$M1S_{2B}^{finite}(N^3LO)$	-4.322	-4.293	-4.117	-3.611	-2.802
$M1S_{2B}^{finite}(N^4LO)$	2.658	3.095	2.709	2.049	1.327
$M1S_{2B}^{finite}$	-1.664	-1.198	-1.408	-1.562	-1.475
$M1S_{1B} + M1S_{2B}^{finite}$	-5.961	-5.494	-5.704	-5.859	-5.772
M1S	-2.849	-2.850	-2.852	-2.856	-2.861

Table 1: Individual contributions to M1S in unit of 10^{-3} fm. $M1S_{2B}^{finite}$ is the sum of $M1S_{2B}^{finite}(N^3LO)$ and $M1S_{2B}^{finite}(N^4LO)$, while $M1S_{2B}^{finite}(N^3LO)$ is the sum of the contributions from the WZ term, $M1S_{2B}^{WZ}(N^3LO)$, and the “fixed-term,” $M1S_{2B}^{fixed}(N^3LO)$. We also list the results in the hard-core cutoff scheme (HCCS) (without the g_4 contribution), $M1S_{1B} + M1S_{2B}^{finite}$, with $M1S_{1B} = -4.297 \times 10^{-3}$ fm. The last row gives the total M1S resulting from the MHCCS regularization.

where the error bar stands for the r_c -dependence. It is highly noteworthy that the r_c -independence holds even when g_4 changes by a factor of ~ 26 .

We also observe that the individual contributions coming from N^3LO and N^4LO are of the same order as the LO one-body contribution. This feature can be traced to the aforementioned facts that the LO one-body contribution is suppressed by the orthogonality of the wavefunctions, and that the N^3LO is suppressed due to the smallness of g_ρ . About half of the N^3LO contributions are cancelled by the N^4LO contributions. In obtaining the above numerical results, we used the KSRF value, $g_\rho \simeq 5.85$, for the ρNN coupling constant featuring in the Wess-Zumino term. If instead we use a more conventional value, $g_\rho \simeq 5.25$, then the resonance-exchange contribution decreases, leading to a larger cancellation between the loop contribution and the N^3LO contributions. Even with the use of a unrealistically small value of the g_ρ which would cause a complete cancellation among the 2-body terms, we have found $M1S = -2.91 \times 10^{-3}$ fm (for the entire range of $0.01 \text{ fm} \leq r_c \leq 0.8 \text{ fm}$), which differs only about 2 % from M1S in Table 1. We note that the MEC contribution reduces the one-body contribution by about 30 %.

The two-body contribution to the E2S turns out to be quite small, $E2S_{2B} = (0.00 \pm 0.01) \times 10^{-3}$ fm for the whole range of $r_c = (0.01 \sim 0.8)$ fm. Combining the one-body and two-body contributions, we obtain

$$E2S = (1.40 \pm 0.01) \times 10^{-3} \text{ fm.} \quad (45)$$

Correspondingly, the two-body contribution to the deuteron quadrupole moment also is quite small, $Q_{d,2B} = -0.002 \text{ fm}^2$. This means that the discrepancy between the experimental value (0.286 fm^2) and the one-body contribution (0.273 fm^2) cannot be explained in terms of the two-body effects as calculated here.

We now discuss briefly the possibility of another renormalization scheme. Earlier, we invoked eq.(36) to eliminate the contribution of the V_1 term. However, if we use a non-zero value of r_c , the delta-function gets smeared and therefore the V_1 term can have a finite contribution even though suppressed by powers of Qr_c . One then might wonder if there exists a possibility to renormalize the deuteron quadrupole moment Q_d as well as the magnetic moment by adjusting V_1 . This is indeed possible, and we shall refer to this scheme as MHCCS*. Since the extension of MHCCS to MHCCS* is straightforward, we simply quote the results. For the range of $r_c = (0.01 \sim 0.8)$ fm, we find $M1S = -2.867(1) \times 10^{-3}$ fm and $E2S = 1.348(0) \times 10^{-3}$ fm. Thus MHCCS* and MHCCS give very similar results. We have found that, as far as the observables are concerned, the MHCCS* results exhibit even a higher degree of insensitivity to r_c than those of MHCCS. Meanwhile, the values of V_1 and g_4 in MHCCS* vary as $V_1 = (3.1 \times 10^5 \sim 24.4)$ fm³ and $g_4 = (5.05 \sim -0.09)$ fm⁴, when r_c changes from 0.01 fm to 0.8 fm. While neither V_1 nor g_4 is an observable, the occurrence of these large coefficients^{#10} as well as the huge variation of V_1 with respect to r_c is rather offending to the *naturalness* of the theory. So we will not consider this scheme seriously.

To illustrate the convergence of our chiral expansion, we also present the results that are renormalized only up to N³LO. To this order, there are no loops, and E2S does not receive any two-particle contribution. The results for M1S again turn out to be very close to what we obtained in MHCCS, exhibiting little r_c -dependence: For $0.01 \text{ fm} \leq r_c \leq 0.8 \text{ fm}$,

$$M1S = (-2.84 \pm 0.01) \times 10^{-3} \text{ fm}. \quad (46)$$

5 Discussion

The only “isospin-violating” effect that features in the above consideration is the trivial fact that the two-nucleon system can emit both isovector and isoscalar photons. We examine here whether any significant additional isospin-violating effects can arise due to higher-order electromagnetic (EM) interactions, or isospin impurity in the two-nucleon system. Although in normal circumstances these effects give only minor corrections, they might be important in calculating highly suppressed amplitudes such as M1S and E2S. It is particularly important to assess those isospin-violating effects in the dominant M1V which mock the isoscalar amplitude. First, we argue that isospin violation in the initial- and final-state interactions cannot influence the observables of our concern. To produce any spin-dependent effects, the initial np state must have $J \neq 0$, and hence, at threshold, should be a 3S_1 state. If this state could be mixed with 1S_0 (the only other available state at threshold), then the dominant M1V transition connecting 1S_0 and the deuteron would produce a rather significant correction to the genuine M1S. In the two-nucleon systems, however, the conservation of J dictates that, even in the presence of isospin-violating inter-

^{#10} From eqs.(33, 34), we can infer that the *natural scales* of the V_1 and g_4 are $N_1 m_\pi \simeq 0.09 \text{ fm}^3$ and $N_{WZ} \simeq 0.03 \text{ fm}^4$, respectively.

actions, there be no mixing between the 1S_0 and 3S_1 channels. Next, we need to examine radiative corrections to the M1 operator itself. Instead of considering all possible diagrams, we study here a typical diagram just to get a rough estimate. One of the diagrams that give non-vanishing corrections is obtained from Fig. 3b by replacing the one-pion line in it with a photon line. Let ξ_{EM} be the ratio of the contribution of this radiative correction diagram to that of Fig. 3b. The EM correction becomes more (less) important for lower (higher) momentum transfers. When the momentum transfer is of order of m_π , we find $\xi_{\text{EM}} \sim \alpha/\alpha_\pi \simeq 0.09$, where $\alpha_\pi \equiv \frac{g_A^2 m_\pi^2}{16\pi f_\pi^2} \simeq 0.08$ ($f_\pi \simeq 93$ MeV). Applied to a specific case of M1S, however, this ratio is enhanced by $\mu_V/\mu_S \simeq 5.3$, as the isovector γNN vertex can contribute to the isoscalar current due to the isospin breaking EM interaction, and as a result the ratio of the EM correction becomes $\sim 1/2$. Thus the EM correction might be substantial compared to the N⁴LO. We remark, however, that, in MHCCS (and also in MHCCS*), this amount of correction would cause negligible changes in the final results.

To conclude, we recapitulate our predictions in the MHCCS scheme for the ratios of the relevant matrix elements and the polarization observables:

$$\begin{aligned}\mathcal{R}_{\text{M1}} &= (-0.49 \pm 0.01) \times 10^{-3}, \\ \mathcal{R}_{\text{E2}} &= (0.24 \pm 0.01) \times 10^{-3},\end{aligned}\tag{47}$$

and strictly at threshold

$$P_\gamma = (-1.04 \pm 0.01) \times 10^{-3},\tag{48}$$

$$\eta_\gamma = 0.80 \pm 0.02,\tag{49}$$

where the errors represent the variance among MHCCS, MHCCS* and the N³LO MHCCS. The r_c -dependences are negligible. The above values of P_γ and η_γ are for complete polarization; that is, $|\vec{P}_n| = 1$ for P_γ and $pP = 1$ for η_γ . As noted, η_γ decreases rapidly when pP becomes smaller; for instance, $\eta_\gamma(pP = 0.96) = 0.62 \times 10^{-5}$ and $\eta_\gamma(pP = 0.25) = 0.86 \times 10^{-7}$.

The results with HCCS are rather different^{#11},

$$\text{HCCS : } \mathcal{R}_{\text{M1}} = (-0.98 \pm 0.03) \times 10^{-3},\tag{50}$$

$$P_\gamma = (-1.73 \pm 0.05) \times 10^{-3},\tag{51}$$

$$\eta_\gamma = 0.53 \pm 0.01,\tag{52}$$

where, this time, the errors reflect the r_c -dependence. The E2S remains the same as in eq.(47).

The presently available experimental data for P_γ [10] is:

$$P_\gamma^{\text{exp}} = (-1.5 \pm 0.3) \times 10^{-3}.\tag{53}$$

^{#11}These differ from the results given in [8] due to the term M1S_{2B}^{fixed} (N³LO) overlooked in the preliminary calculation reported there.

Although the prediction in the HCCS, (51), gives a P_γ closer to (53), we regard our MHCCS result (47) to be more reliable. The results of Chen, Rupak and Savage [2] for the ratios \mathcal{R}_{M1} and \mathcal{R}_{E2} computed in the PDS counting scheme of [12] are quite close to ours (47). Even with the rather generous error estimates in [2] taken into account, this agreement is remarkable.^{#12}

While we believe that MHCCS is more reliable than HCCS, we should note that the MHCCS and HCCS results for \mathcal{R}_{M1} differ by a factor of ~ 2 . To be conservative, we should take this difference as uncertainty in the treatment of the short-distance physics involved. (\mathcal{R}_{E2} does not distinguish the two hard-core cutoff schemes.) This sort of uncertainty was implied in the chiral filter hypothesis of ref.[4]. It has been mentioned in various places that, when protected by the chiral filter, the HCCS procedure yields quantitatively accurate results. But the other side of the coin of the chiral filter suggests that the HCCS procedure is likely to fail when unprotected by the chiral filter, as in the case of the isoscalar matrix elements at hand. Our results here indicate how to understand the possible demise of the much used hard-core cutoff procedure, a procedure which has long been a standard method in nuclear physics, in terms of an effective field theory regularization. What comes out as a surprise from this work is that, despite the uncertainty due to the short-distance behavior, one can make a reasonably quantitative calculation of the observables that are *not* protected by the chiral filter mechanism. We await with great eagerness the forthcoming results of the ILL experiment, which will bring crucial information on this issue.

Acknowledgments

We would like to thank Thomas M. Müller for informing us of his experiment in progress and for useful discussions and Martin Savage for demonstrating to us the predictive power of the effective field theory approach he and his co-workers have developed. We are grateful to C.W. Kim, Director of KIAS, for the hospitality and encouragement at KIAS where this work was completed. The work of KK was partially supported by the NSF Grant No. PHYS-9602000, and that of DPM by the KOSEF through CTP of SNU and by the Korea Ministry of Education contract No. 98-2418.

References

- [1] T.M. Müller, private communication; T.M. Müller, D. Dubbers, P. Hautle and O. Zimmer, “Measurement of the γ anisotropy in the $\vec{p}\vec{n}, \gamma d$ -process,” in the Proceedings of the “International Workshop on Particle Physics with Slow Neutrons,” ILL, Grenoble, France, 22-24 October, 1998.
- [2] J.-W. Chen, G. Rupak and M.J. Savage, “Suppressed amplitudes in $np \rightarrow d + \gamma$,” nucl-th/9905002.

^{#12} Thus the challenge made in [8] was quickly met by these authors.

- [3] G. Breit and M.L. Rustgi, Nucl. Phys. A **161** (1971) 337.
- [4] K. Kubodera, J. Delorme and M. Rho, Phys. Rev. Lett. **40** (1978) 755.
- [5] M. Rho, Phys. Rev. Lett. **66** (1991) 1275. .
- [6] T.-S. Park, D.-P. Min and M. Rho, Phys. Rev. Lett. **74** (1995) 4153. ; Nucl. Phys. A **596** (1996) 515.
- [7] A.E. Cox, S.A.R. Wynchank and C.H. Collie, Nucl. Phys. **74** (1965) 497.
- [8] T.-S. Park, K. Kubodera, D.-P. Min and M. Rho, “On making predictions with effective field theories in nuclear physics,” nucl-th/9904053
- [9] G.P. Lepage, talk given at the Workshop on “Nuclear Physics with Effective Field Theories,” INT, University of Washington, February 25-26, 1999.
- [10] A.N. Bazhenov *et al*, Phys. Lett. B **289** (1992) 17.
- [11] S. Weinberg, Phys. Lett. B **251** (1990) 288. ; Nucl. Phys. B **363** (1991) 3. ; Phys. Lett. B **295** (1992) 114.
- [12] D.B. Kaplan, M. Savage and M. Wise, Nucl. Phys. B **478** (1995) 629. ; Phys. Lett. B **424** (1998) 390. ; Nucl. Phys. B **534** (1998) 329. ; Phys. Rev. C **59** (1999) 617.
- [13] R.B. Wiringa, V.G.J. Stoks and R. Schiavilla, Phys. Rev. C **51** (1995) 38.
- [14] T.-S. Park, K. Kubodera, D.-P. Min and M. Rho, Phys. Rev. C **58** (1998) R637. ; Nucl. Phys. A **646** (1999) 83.
- [15] U. van Kolck, “Effective field theory of nuclear forces,” nucl-th/9902015
- [16] M. Savage, K.A. Scaldeferri and M.B. Wise, nucl-th/9811029
- [17] N. Fettes, U.-G. Meissner and S. Steinberg, Nucl. Phys. A **640** (1998) 199.
- [18] G. Arfken, “Mathematical Methods for Physicists”, Academic Press, New York, 3rd ed. 1985.
- [19] D.B. Kaplan and J.V. Steele, “The long and short of nuclear effective field theory expansions,” nucl-th/9905027, and references given therein.